

# Vertical transport of ozone and CO during super cyclones in the Bay of Bengal as detected by Tropospheric Emission Spectrometer

S. Fadnavis · G. Beig · P. Buchunde · Sachin D. Ghude · T. N. Krishnamurti

Received: 22 February 2010 / Accepted: 5 July 2010 / Published online: 21 July 2010  
© Springer-Verlag 2010

**Abstract** Vertical profiles of carbon monoxide (CO) and ozone retrieved from Tropospheric Emission Spectrometer have been analyzed during two super cyclone systems Mala and Sidr. Super cyclones Mala and Sidr traversed the Bay of Bengal (BOB) region on April 24–29, 2006 and November 12–16, 2007 respectively. The CO and ozone plume is observed as a strong enhancement of these pollutants in the upper troposphere over the BOB, indicating deep convective transport. Longitude–height cross-section of these pollutants shows vertical transport to the upper troposphere. CO mixing ratio ~90 ppb is observed near the 146-mb level during the cyclone Mala and near 316 mb during the cyclone Sidr. Ozone mixing ratio ~60–100 ppb is observed near the 316-mb level during both the cyclones. Analysis of National Centers for Environmental Prediction (NCEP) reanalysis vertical winds (omega) confirms vertical transport in the BOB.

**Keywords** Ozone · CO vertical transport during super cyclones · Tropospheric emission spectrometer

## 1 Introduction

Over the past two decades, study of transport of ozone and its precursors in the upper troposphere has accelerated due

to the advancement in satellite measurements and model simulations. The upper troposphere is a region important for chemistry and dynamics because of its distance from the source region near Earth's surface and its proximity to the tropopause (Mahlman 1997). This is the region where radiative forcing, long-range pollution transport, and the transport of air into/from the stratosphere play important role. The three-dimensional models indicate that the dominant mechanism for exchanging air between Northern and Southern hemispheres mostly operate in the tropical upper troposphere (Tans et al. 1990). The mechanisms for lifting trace gases out of the Planetary Boundary Layer (PBL) into the free troposphere is key in understanding the local air pollution problem as well as regional and global atmospheric chemistry and climate issues (Dickerson et al. 2007). Convection and orographic flow can be important for lifting of pollution out of the boundary layer (Liu et al. 2003; Henne et al. 2004; Hess 2005; Ding et al. 2009). Cyclones play a dominant role in tropospheric trace gas transport to the middle and upper troposphere. A good understanding of trace gas transport from low levels to the free troposphere is needed since polluted air lifted to higher altitudes can perturb natural chemical cycles and may impact the global radiation budget, which in turn may affect air quality at distant downstream locations (Kiley and Fuelberg 2006).

A number of studies on midlatitude cyclones and their effects on pollution transport have been reported in the past (Ding et al. 2009; Miyazaki et al. 2003; Cooper et al. 2004; Liang et al. 2004; Dickerson et al. 2007). Some of these studies have shown that warm conveyor belt (WCB) can lift pollution plumes into the upper troposphere. Quite a few studies are focused on the role of the tropical deep convective system in transporting pollutant (Jenkins et al. 2008, Bellevue et al. 2007, Andreae et al. 2001). The

---

Responsible editor: Euripides Stephanou

---

S. Fadnavis (✉) · G. Beig · P. Buchunde · S. D. Ghude  
Indian Institute of Tropical Meteorology,  
Pune, India  
e-mail: suvarna@tropmet.res.in

T. N. Krishnamurti  
Department of Meteorology, Florida State University,  
Tallahassee, FL, USA

connection between the upper and lower troposphere in the equatorial region is fast and efficient because of the dominant role of moist convection. The Bay of Bengal (BOB) is relatively more polluted region, because it is more strongly influenced by surrounding continental emissions than the Arabian Sea, with the pollution originating mainly from Indian and Southeast Asian outflow during most of the year and China during part of the year (Lelieveld et al. 2001; Kunhikrishnan and Lawrence 2004; Kunhikrishnan et al. 2004). Lelieveld et al. (2001) also reported that over the BOB, most observed pollutants are from the Gangetic plains of India and transported via Indo-Gangetic Plume. From Geophysical Fluid Dynamics Laboratory model simulation, Phadnis et al. (2002) reported transport of ozone,  $\text{NO}_x$ , and CO over the Indian Ocean during winter–spring monsoon (January–February–March). They reported that Southeast Asian emissions have the greatest impact over the BOB. These pollutants are transported into the upper troposphere by convection events (Kar et al. 2004). Convective lifting of the transported pollution supplies ~10% of the ozone over the Indian Ocean in the tropical upper troposphere (Phadnis et al. 2002). Further, Krishnamurti et al. (1997) carried out passive tracer studies during the winter monsoon. They identified three major regions of inflow to the Intertropical Convergence Zone (ITCZ): the Arabian Sea, the BOB, and Southeastern Indian Ocean (Ramana and Ramanathan 2006). This equator ward monsoonal flow over the North Indian Ocean into the convectively active ITCZ provides an efficient mechanism for transporting surface pollution from South Asia into the tropical upper troposphere/lower stratosphere where, because of stronger winds and longer lifetimes, rapid long-range transport can occur (Krishnamurti et al. 1997). Ozone in the middle and upper troposphere has several sources: It may come from surface via upward transport, or from the stratosphere via downward transport, or from lightning production. During stratospheric intrusion, ~200–300 ppb of ozone mixing ratios are observed in the upper troposphere (Kim et al. 2002), while during vertical transport, ozone mixing ratios ~90–120 ppb are observed in the upper troposphere (Jenkins et al. 2008).

Increasing levels of greenhouse gases as well as aerosols in the Earth's atmosphere are likely to be direct consequence of human activities (IPCC 2007). These anthropogenic activities lead to emission of CO,  $\text{NO}_x$ , and VOCs, which generate tropospheric ozone (Phadnis et al. 2002). These pollutants are known to modify global tropospheric composition. Anthropogenic emissions of various pollutants in Asia are increasing because of rapid industrialization and urban development (Streets and Waldhoff 2000; Streets et al. 2003). Industrialization of eastern Asia influences chemical climate of India through transport processes and thus Indian monsoon (Krishnamurti et al. 2009). Transport of these

emissions has been observed to alter the distributions of various trace gases over the Indian Ocean (Lelieveld et al. 2001, and references therein). In particular, elevated levels of pollutants have been observed over the Indian Ocean, when air masses were transported via BOB. These surface pollutants are episodically lifted into the upper troposphere by tropical convection events (Phadnis et al. 2002).

The aim of this article is to study the role of the super cyclones in the transport of ozone and carbon monoxide in the upper troposphere. To achieve this goal, we have analyzed profiles of ozone and CO retrieved from Tropospheric Emission Spectrometer (TES) during two typical tropical super cyclones traversed the Bay of Bengal (BOB). The cyclone Mala (April 25–29, 2006) and Sidr (November 12–16, 2007) traversed the BOB during premonsoon and postmonsoon seasons. The vertical profiles retrieved from TES provide information of distribution of CO and ozone from the lower troposphere to the upper troposphere. Here we report CO and ozone plume in the upper troposphere as evidence of deep convection during a super cyclone.

## 2 Data and method

### 2.1 Satellite and reanalysis data

The TES launched into sun-synchronous orbit aboard Aura, the third of NASA's Earth Observing System (EOS) spacecraft, on July 15, 2004. TES provides a global view of tropospheric trace gas profiles including ozone, water vapor, and carbon monoxide, along with atmospheric temperature, surface temperature and emissivity, effective cloud top pressure, and effective cloud optical depth (Worden et al. 2004). TES latitudinal extent is from 82°S to 82°N and longitude range is 0°–360°. For cloud-free conditions, the vertical resolution of TES ozone profile retrievals is typically 6 km in the tropics (Worden et al. 2004; Jourdain et al. 2007). TES measurements are available since 2005. TES level 2 data with grid spacing 4° longitude × 2° latitude are analyzed in the present study. Tropospheric ozone retrievals from TES have been validated against ozonesonde and lidar measurements, and it is generally found that the values are biased high by as much as 15% after accounting for the TES vertical resolution (Worden et al. 2009). TES ozone and CO mixing ratios are obtained from the Web site: <ftp://14ftl01.larc.nasa.gov/TES/TL2O3N.003>

Spatial distribution of TES ozone and CO mixing ratios are studied over the BOB region (8–22°N, 80–100°E) for the days of occurrence of cyclone Mala (25–29 April 2006) and Sidr (on November 12–16, 2007). Spatial distribution of ozone and CO at tropospheric pressure levels (825, 681, 464, 316, 215, 146, 100 mb) are analyzed in order to study their vertical transport.

National Centers for Environmental Prediction (NCEP) reanalysis II winds and vertical winds (omega) are analyzed at every pressure level between 1,000 and 100 mb. Plots of winds at 500, 300, and 150 mb are incorporated in the present study to show circulation pattern.

## 2.2 Meteorological overview of super cyclones

### 2.2.1 Super cyclone Mala

Tropical cyclone Mala formed in the BOB on April 24, 2006 (the premonsoon period). An area of convection persisted over the southern BOB in mid- to late April and organized around a low level circulation. On April 23, convection built around the system and consolidated around the center. The area continued to organize and was upgraded to deep depression on the April 25. The deep depression moved to the northwest and intensified into a cyclonic storm Mala later that day. Mala intensified into a severe cyclonic storm on April 27. On April 28, Mala further rapidly intensified to category 4 cyclone. Figure 1 exhibits the track of cyclone Mala.

### 2.2.2 Super cyclone Sidr

Cyclone Sidr traversed the BOB region on November 12–16, 2007 (postmonsoon period). On November 9, 2007, an air mass disturbance with weak low-level circulation begun to develop in the central BOB. On November 11, 2007, a better defined cyclonic circulation developed. Later that day, the system was designated as a tropical depression. On November 11, system was upgraded to tropical cyclone. On November 12, 2007, it was further upgraded to a severe cyclonic storm and named “Sidr.” On November 15, 2007,

it strengthened to reach category 4 tropical cyclone. On November 16, center of Sidr was located at 19°N, 90°E. Figure 2 depicts the track of cyclone Sidr.

## 2.3 Studied region

Figure 3 depicts the map of India. In the present study, the Bay of Bengal (BOB) region is considered as 8–22°N, 80°–100°E. During the passage of cyclones Sidr and Mala, low-pressure areas were formed over the Indian region. On April 28, 2006 (during cyclone Mala), low-pressure area formed over Chattisgarh-Orissa region, and on November 15, 2007 (during cyclone Sidr), it was near Ratnagiri coast. These regions are indicated by circles in Fig. 3. Indo-Gangetic plain and Mumbai-Gujrat industrial region are highly polluted due to the large number of thermal power plants, steel plants, cement plants, and other industries clustered in this region (Ghude et al. 2008). Under favorable meteorological conditions, the pollutants from Indo-Gangetic belt influence the pollutants in the BOB via Indo-Gangetic plume (Kunhikrishnan and Lawrence 2004), and pollutants from Mumbai-Gujrat industrial region are transported to nearby area. These regions are marked by rectangular strip. In the discussion that follows, we considered seasons as premonsoon (March–April–May), summer monsoon (June–July–August–September), and postmonsoon (October–November–December).

## 3 Results and discussions

In order to study the effect of super cyclones on the distribution of pollutants CO and O<sub>3</sub>, their latitude–longitude cross-section is examined at seven pressure levels between 825 and 100 mb. Latitude–longitude distribution

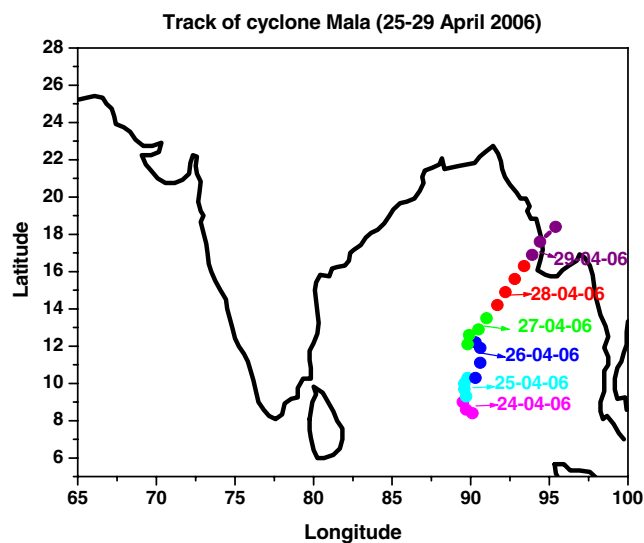


Fig. 1 The track of cyclone Mala on April 25–29, 2006

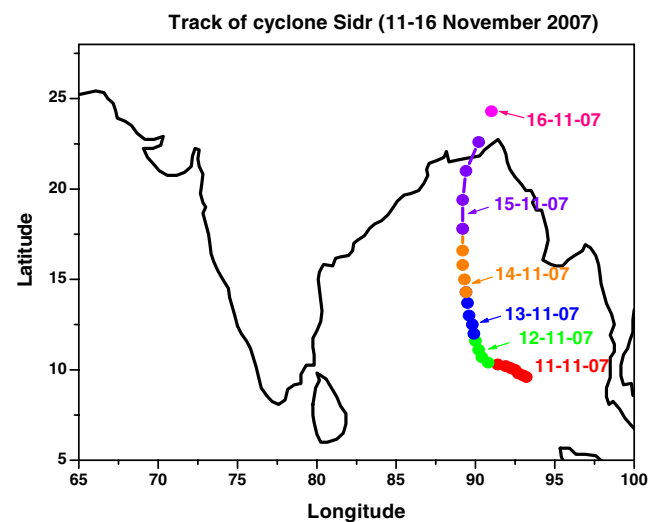
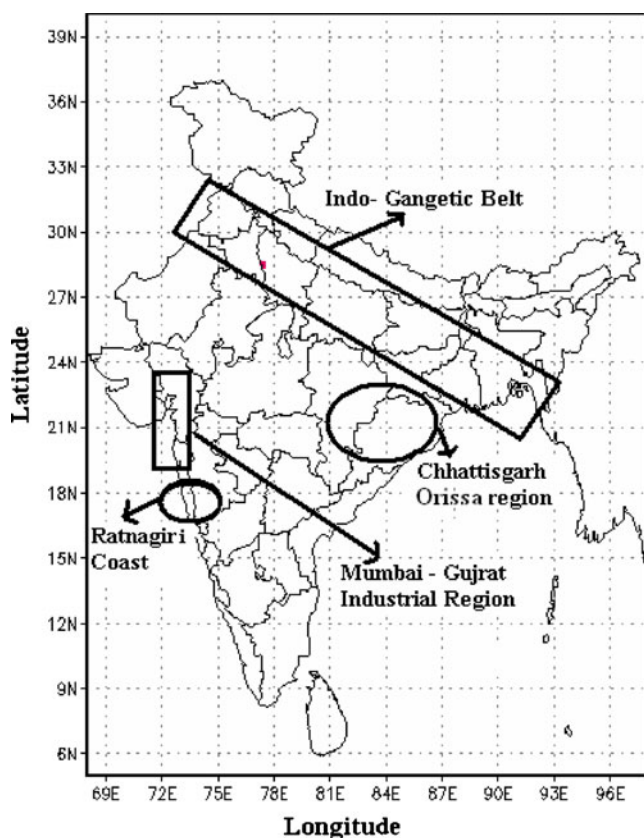


Fig. 2 The track of cyclone Sidr on November 11–16, 2007



**Fig. 3** Map of India indicating low-pressure areas near Ratnagiri coast, Chhattisgarh-Orissa region (indicated by circles), Indo-Gangetic belt, Mumbai Gujrat region (marked by rectangular strips)

of ozone and CO is plotted for the days of cyclone Mala (April 25–29, 2006) and Sidr (November 12–16, 2007). Here are shown only the plots for the days on which the cyclone intensity was greatest (category 4): April 28, 2006 for the Mala cyclone and November 15, 2007 for the Sidr cyclone. Distribution of CO and ozone on other days of cyclones is similar to these days with small variation in magnitude. In the present study, distribution of ozone and CO is shown over the wider area (8–28°N, 64–100°E) in order to visualize their distribution in the surrounding area.

### 3.1 Spatial distribution of O<sub>3</sub> in the BOB during super cyclone Mala

Figure 1 depicts the position of cyclone Mala on April 28, 2006. Latitude–longitude cross-section of distribution of ozone over the BOB and surrounding area on April 28 at different tropospheric pressure levels (825, 681, 464, 316 mb) is shown in Figs. 4a–d. Spatial distribution of ozone at 825-mb level shows two maximum (>130 ppb): one near the location of cyclone Mala and another over Chhattisgarh-Orissa region. During the cyclone, strong winds gushing into the cyclone transport pollutants and trace gases from the surrounding area to the cyclone.

Hence, enhanced ozone mixing ratios are observed near the location of cyclone. In order to investigate the reason for the maximum over the continent, Indian daily weather map for the surface pressure was analyzed for April 28, 2006 (IDWR 2006) as can be seen in Fig. 5. This weather map shows a low-pressure area over the Chhattisgarh-Orissa region, which could explain observed ozone maximum over this region. Higher ozone mixing ratios might have been transported from the Indo-Gangetic region to the region of low-pressure area and cyclone. Hence, ozone mixing ratios over these regions are high. During premonsoon season, biomass burning activity is also high in the Indo-Gangetic region, contributing to the emission of ozone precursor pollutants such as NO<sub>x</sub> and CO. Moreover, favorable meteorological conditions and higher actinic conditions eventually lead to more ozone production (Beig and Ali 2006; Ghude et al. 2008). The ozone maximum over the Chhattisgarh-Orissa region is widespread as compared with maximum near the location of cyclone. The reason may be that generally, the ozone mixing ratios over the Indian landmass are more than that of the ocean; moreover, this region is near to the Indo-Gangetic plains. The Indo-Gangetic plume (containing higher ozone mixing ratios in premonsoon season) might have contributed in enhancing ozone in this area. The ozone mixing ratios ~100 ppb are observed near the head bay (87–93°E, 18–22°N). Figure 4b shows spatial distribution of ozone at 681-mb level. The ozone maximum near the location of cyclone is clearly seen. Another maximum appear near the head bay. This may be related to the orographic flow of cyclonic winds. Ozone mixing ratios ~100–110 ppb are observed near the head bay and location of cyclone. Figure 4c, d shows spatial distribution of ozone at 464- and 316-mb level. Ozone maximum ~75 ppb is observed at 464 mb and 65 ppb at 316-mb level over the BOB. Spatial distribution of ozone at 215 mb (figure not shown) shows ozone mixing ratios ~60 ppb near the location of cyclone. Strong lightning activity during the cyclone contributes in photochemical production of ozone (via NO<sub>x</sub>) in the upper troposphere. This may contribute in enhancing ozone mixing ratios near the location of cyclone. The spatial distribution of ozone at 146-mb pressure level does not show such enhancement near the location of cyclone (figure not shown).

In order to study vertical transport, ozone mixing ratios are averaged over the BOB latitudes 8–22°N. The longitude–altitude cross-section of ozone mixing ratios is shown in Fig. 4e. The vertical transport of ozone over the BOB longitudes (80–110°E) is quite evident. Ozone mixing ratios ~65 ppb are observed near 316-mb pressure level. Vertical winds (omega) obtained from NCEP reanalysis data are averaged over the latitudes 8–22°N. The longitude–altitude cross-section (Fig. 4f) of omega shows strong

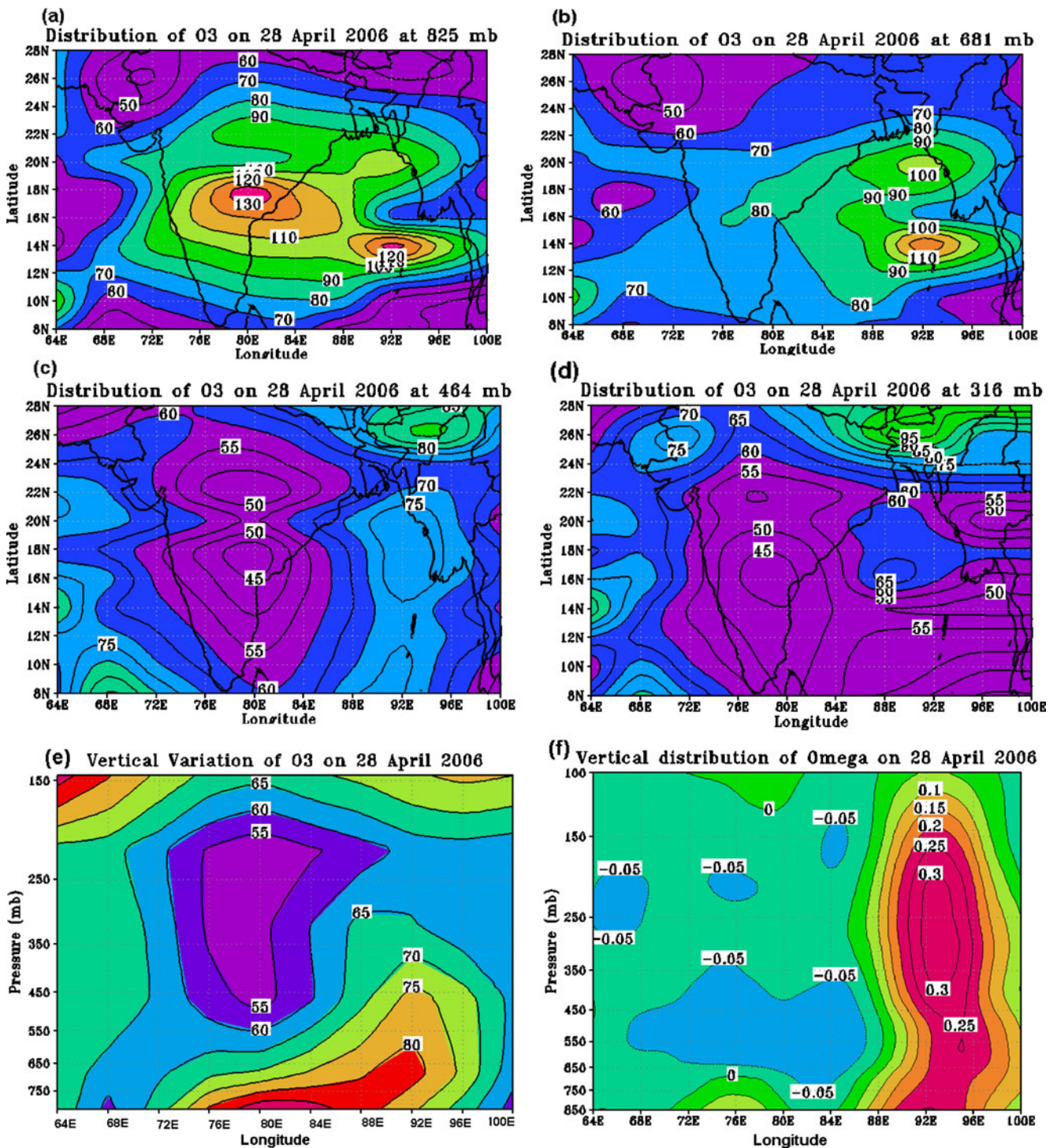


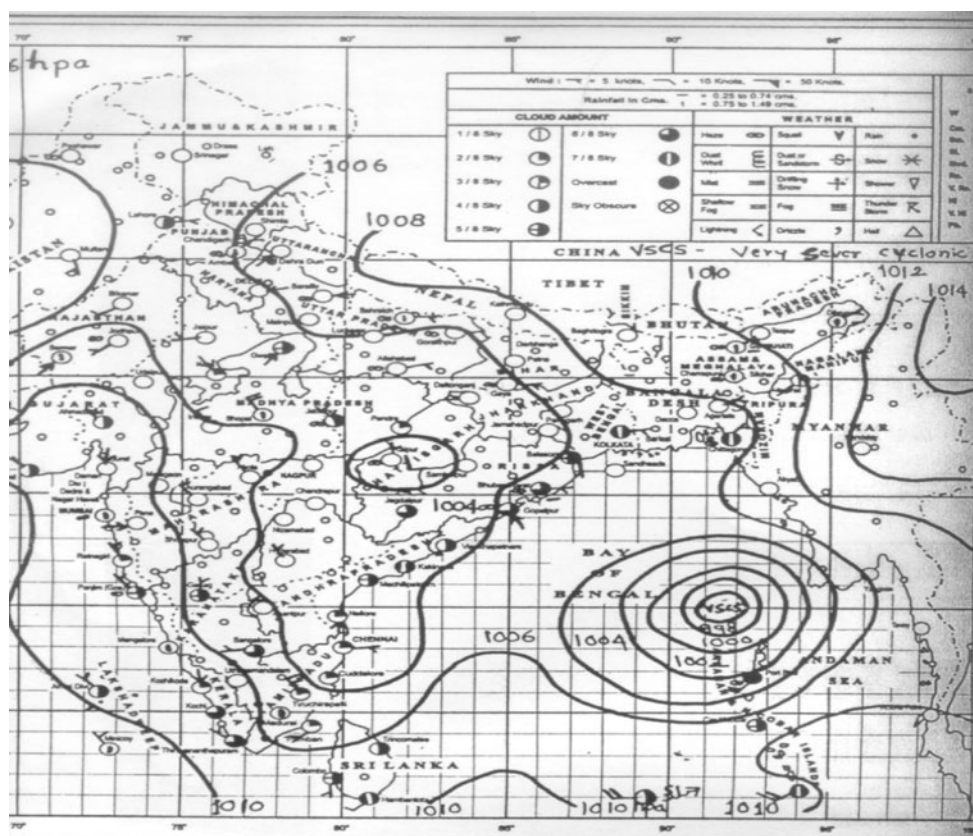
**Fig. 4** Spatial distribution of TES ozone on April 28, 2006 at **a** 825 mb, **b** 681 mb, **c** 464 mb, and **d** 316 mb. **e** Longitude–height cross-section (mean for latitudes 8–22°N) of TES ozone on April 28,

2006. **f** Longitude–height cross-section (mean for latitudes 8–22°N) of NCEP reanalysis vertical winds (omega) on April 28, 2006

convection over the BOB longitudes (80–100°E). Strong convection during cyclone might have lifted lower tropospheric ozone to 316-mb level. It is interesting to note that between the longitudes 64–70°E, there seems to be a vertical gradient of ozone (Fig. 4e), with higher mixing

ratios in the upper troposphere. This may be due to downward transport from the stratosphere or due to lightning production. Figure 4f shows negative omega for the same region. This indicates that a downward transport of ozone might have occurred. Over the Indian region, the

**Fig. 5** Spatial distribution of surface pressure on April 28, 2006 (IDWR 2006)



evidence of stratospheric intrusion during the passage of tropical cyclone is also reported by Das (2009).

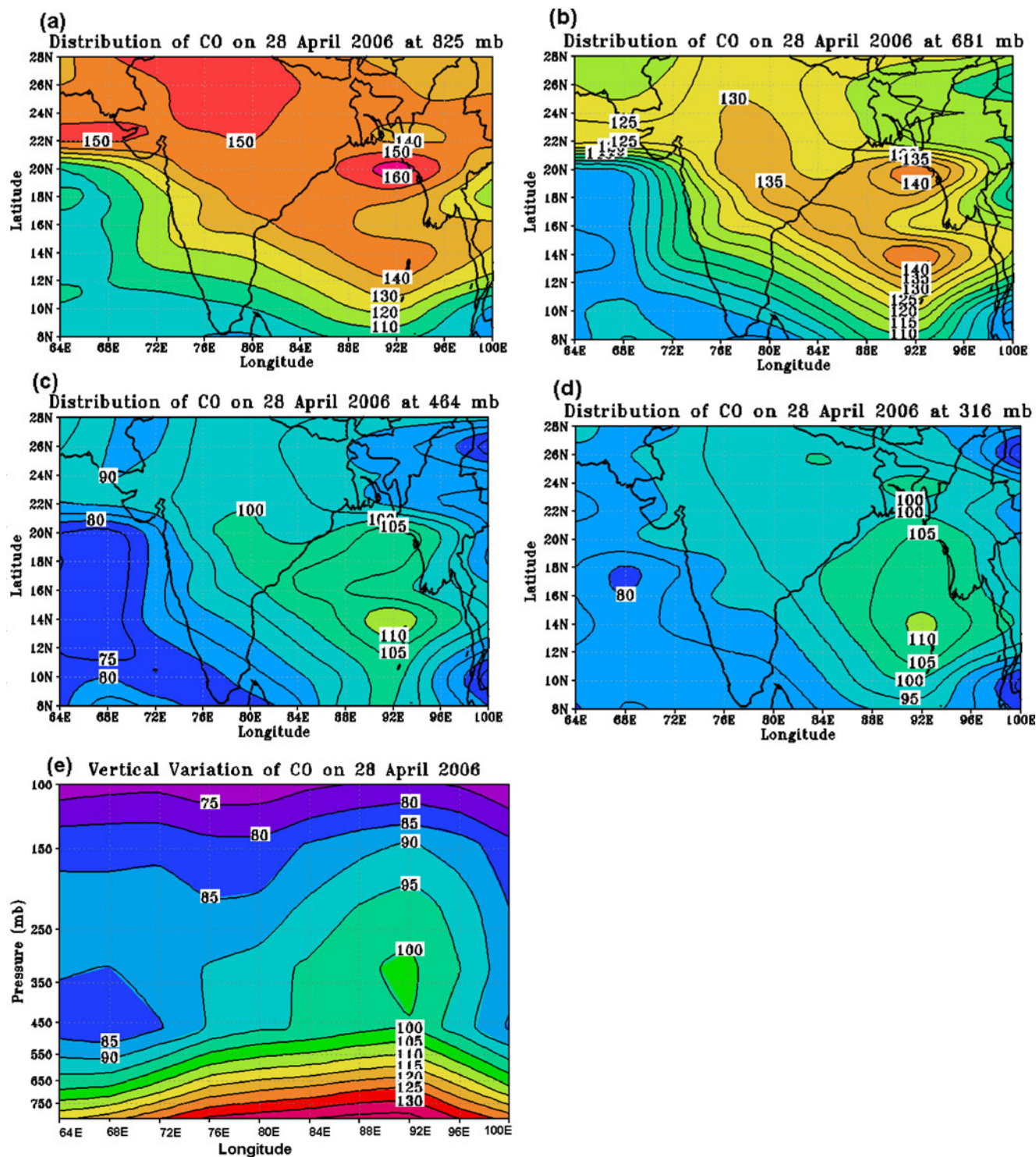
### 3.2 Spatial distribution of CO in the BOB during super cyclone Mala

Figure 6a–d exhibits latitude–longitude cross-section of CO on April 28, 2006, at 825-, 681-, 464-, and 316-mb pressure levels. The CO mixing ratios  $\sim 140$  ppb are observed near the location of cyclone and near the low-pressure area (Chattisgarh–Orissa region). The most obvious feature in Fig. 6a is enhanced CO ( $>160$  ppb) near the head BOB ( $\sim 20^\circ\text{N}$ ,  $92^\circ\text{E}$ ). In general, transport from the surrounding landmass (especially from the Indo-Gangetic plains) to the BOB is clearly seen in Fig. 6a. Gushing of the winds from the surrounding area to the cyclone might have transported CO in the BOB as observed in Fig. 6a. The CO maximum near the head bay may be related to the orographic flow of cyclonic winds and longer life time of CO (2–3 months). Distribution of CO at 681 mb is shown in Fig. 6b. The two maximum (CO mixing ratios  $>140$  ppb) are observed: one near the cyclone Mala and another near the head bay. Transport from the Indo-Gangetic plains to the BOB is also seen. Distribution of CO at 464 mb (Fig. 6c) also shows the structure similar to 825- and 681-mb pressure levels. CO mixing ratios  $>110$  ppb is observed near the location cyclone Mala and  $>100$  ppb near the head bay. At 316-mb

pressure level, enhanced CO  $>100$ – $110$  ppb are observed near the location of cyclone Mala. Distribution of CO over at 215 and 146 mb (figures not shown) also shows similar structure with maximum near the location of cyclone Mala. The CO mixing ratios  $\sim 100$ – $110$  ppb are observed at 215 mb and 90–95 ppb at 146-mb pressure level.

In order to understand the vertical distribution, CO mixing ratios are averaged over the BOB latitudes  $8$ – $22^\circ\text{N}$ . The longitude–height cross-section of CO is shown in Fig. 6e. Vertical transport of CO over the BOB longitudes is quite evident. CO mixing ratios  $\sim 90$  ppb are observed near 146 mb. Figure 4f shows strong convection with vertical winds ( $0.2$  Pa/s) extending up to 146-mb pressure level. These strong winds during the cyclone might have lifted CO from the lower troposphere to the upper troposphere ( $\sim 146$  mb) as observed in Fig. 6e. During this cyclone, CO is transported to higher altitudes as compared with ozone. This may be related to longer lifetime of CO (2–3 months) than ozone (weeks to month); also, CO is less reactive than  $\text{O}_3$ . It has only one source, as opposed to tropospheric ozone.

The time series plots of ozone and CO on April 12 and May 6, 2006, at a grid point centered at  $18^\circ\text{N}$ ,  $88^\circ\text{E}$  in the BOB, at pressure levels between 825 and 146 mb, is shown in Fig. 7a, b, respectively. It is quite evident from Fig. 7a that on April 23 to May 2, 2006, ozone mixing ratios are high at 825-, 681-, and 464-mb pressure levels as compared



**Fig. 6** Spatial distribution of TES CO on April 28, 2006 at **a** 825 mb, **b** 681 mb, **c** 464 mb, and **d** 316 mb. **e** Longitude–height cross-section of TES CO (mean for latitudes 8–22°N) on April 28, 2006

with other days. On April 28, ozone maximum (~135 ppb) is observed at 825 mb. Elevated ozone mixing ratios ~125 and ~95 ppb are also observed at 681- and 464-mb pressure levels. Vertical transport of ozone due to convection during cyclone is quite evident. Longitude–altitude cross-section

of ozone (Fig. 4e) shows vertical transport of ozone up to 316 mb. Similarly, time series plots of CO at the same location during the same period also show vertical transport of CO (Fig. 7b). CO mixing ratio is as high as ~140–150 ppb on April 28–30, 2006 at 825- and 681-mb pressure

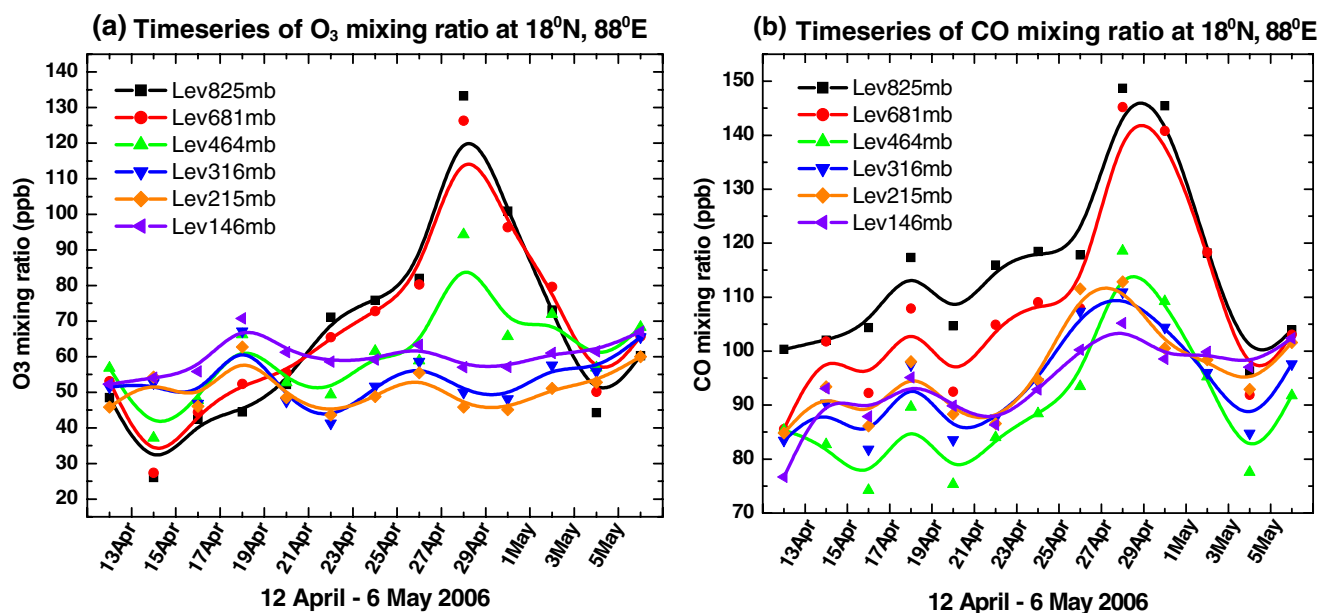


**Fig. 7** Time series plot on April 12, 2006 to May 6, 2006 at 825, 681, 464, 316, 215, and 146 mb at a grid point centered at 18°N, 88°E **a** ozone and **b** CO mixing ratio

levels. Elevated CO mixing ratios (~100–115 ppb) are observed between 464- and 146-mb pressure levels. Longitude–altitude cross-section of CO (Fig. 6e) also exhibits transport from surface to 146-mb pressure level. It is interesting to see the evolution of ozone and CO as the cyclone approaches the chosen grid location. In the BOB as the convection started building up (on April 23, 2006), ozone mixing ratios started increasing at pressure levels between 825 and 464 mb and CO at 825 and 146 mb. From April 24 onwards, as cyclone Mala started approaching the chosen grid location, built up of ozone and CO mixing ratios at the chosen grid location is greater; the closer the cyclone, the higher the ozone (near 825–464 mb) and CO mixing ratios (near 825–146 mb). On April 28, cyclone Mala was nearest to the chosen grid; hence, both ozone and CO mixing ratios were maximum at these levels. After the passage of cyclone, ozone and CO mixing ratio started decreasing.

### 3.3 Spatial distribution of O<sub>3</sub> in the BOB during super cyclone Sidr

Figure 2 depict the location of cyclone Sidr on November 15, 2007. Spatial distribution of ozone on November 15, 2007 at different pressure levels (825–316 mb) is shown in Fig. 8a–d. The most obvious feature is the occurrence of two ozone maxima: one near the location of Cyclone Sidr (Bangladesh–West Bengal region) and another near the Ratnagiri coast (17°N, 73°E) of India. Figure 9 depicts the surface pressure distribution on November 15, 2007 (IDWR 2007). It shows a low-pressure area near the Ratnagiri

coast. Enhanced ozone mixing ratios near the Ratnagiri coast may be related to a low-pressure area. The ozone mixing ratios are more near the Ratnagiri coast (>120 ppb) as compared with that near the location of cyclone (~70 ppb). The reason may be that ozone mixing ratios are generally high over the land as compared with oceans, and another reason may be that this region is near the Mumbai-Gujrat industrial region. This region is the one of the major Large Point Source of pollutants in India (Ghude et al. 2008). During postmonsoon season, there is high concentration of NO<sub>x</sub> (~2–20 ppb) over this region, which leads to high ozone production in this region (Beig and Ali 2006). The pollutants from this Large Point Source get transported to low-pressure area near the Ratnagiri coast. The location of cyclone is near the eastern Indo-Gangetic plains; the Indo-Gangetic plume may contribute in enhancing ozone near the location of cyclone. Ozone mixing ratios ~130 ppb are observed near the location of cyclone. The spatial distribution of ozone at 681 mb is shown in Fig. 8b. Ozone mixing ratios ~100 ppb is observed near Ratnagiri coast and ~120 ppb near the location of cyclone Sidr. It is interesting to observe spatial distribution of ozone at 464- and 316-mb levels (Fig. 8c, d). The horizontal transport of ozone from low-pressure area near the Ratnagiri coast to the region near the location of cyclone is clearly seen. Hence, the O<sub>3</sub> distribution at 316-mb level shows a decrease of ozone mixing ratios near the low-pressure area near Ratnagiri coast and an increase of ozone (~100 ppb) in the region near the location of cyclone Sidr. Strong lightning activity during the cyclone produces ozone via NO<sub>x</sub> in the upper troposphere (Hauglustaine et al. 2001).

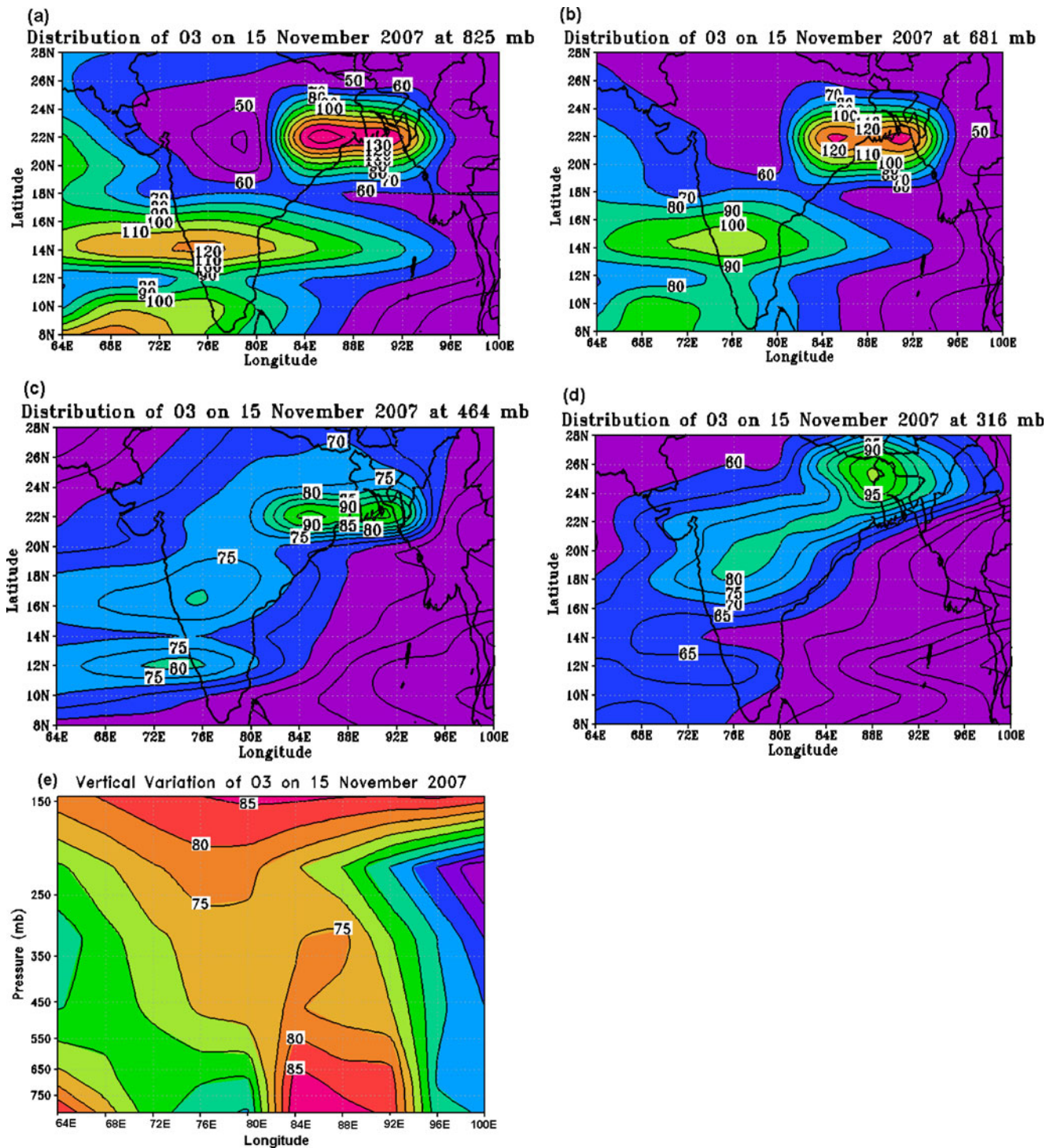
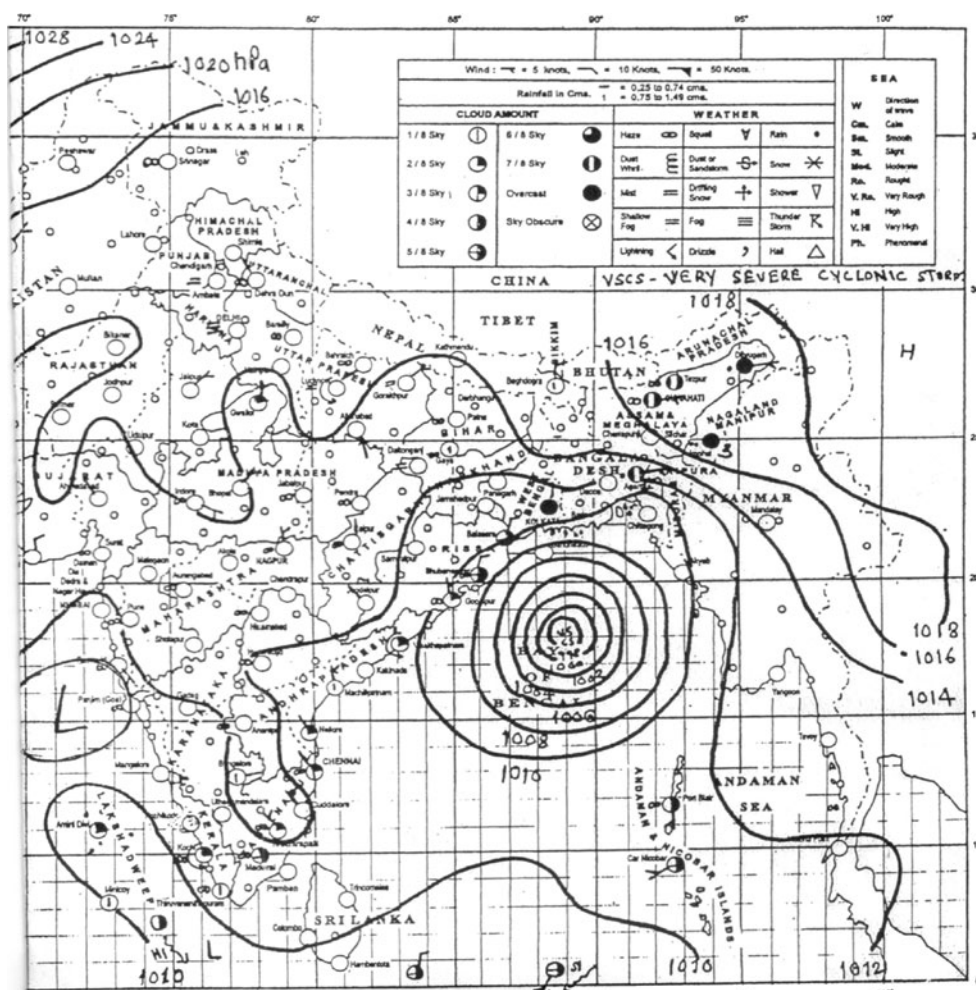


**Fig. 8** Spatial distribution of TES ozone on November 15, 2007 at **a** 825 mb, **b** 681 mb, **c** 464 mb, and **d** 316 mb. **e** Longitude–height cross-section (mean for latitudes 18–24°N) of TES ozone on November 15, 2007

Thus, lightning activity might have been contributed for observed elevated ozone mixing ratio near 316 mb. Spatial distribution of ozone at 215- and 146-mb level (figures not shown) shows ozone maxing ratios ~85 ppb near the location of cyclone. During this cyclone besides direct vertical transport over the BOB region, with the

increase in altitude, ozone mixing ratios from Ratnagiri coast also get transported to the location of cyclone. Hence, averaging over latitudes, the vertical and horizontal transport gets mixed up and vertical transport is not prominent. Hence, to show a clear picture of vertical transport, ozone mixing ratios are averaged only over the

**Fig. 9** Spatial distribution of surface pressure on November 15, 2007 (IDWR 2007)



latitudes covering location of cyclone Sidr (18–24°N). Longitude–altitude cross-section of ozone is shown in Fig. 8e. Ozone plume is observed over the BOB region. Ozone mixing ratios ~75 ppb are observed near 316-mb pressure level. Similar to cyclone Mala, ozone intrusion (longitude 82°E to 93°E) is also seen. Ozone intrusion reaches lower altitudes during cyclone Sidr than cyclone Mala.

### 3.4 Spatial distribution of CO in the BOB during super cyclone Sidr

Figure 10a–d exhibits spatial distribution of CO on November 15, 2007. At 825-mb pressure level (Fig. 10a), similar to ozone distribution, CO also shows two maximums, one near the location of cyclone (west Bengal, Bangladesh, Assam region; >200 ppb) and another (>130 ppb) extending from Arabian sea, Ratnagiri coast, parts of Karnataka, Andhrapradesh, to the BOB. CO mixing ratios are more near the location of cyclone than near the low-pressure area near the Ratnagiri coast. The reason may be the vicinity of cyclone near the eastern part of the Indo-Gangetic plain. The cyclonic

winds may accumulate CO emissions from this area, also during winter–spring season South East Asian plume transport pollutants to the BOB. Thus, enhanced CO near the location of cyclone may be due to Indo-Gangetic plume and Southeast Asian plume. Spatial distribution of CO at 681 mb (Fig. 10b) is similar to 825-mb level. CO mixing ratios ~150 ppb are observed near the location of cyclone. At 464-mb pressure level (Fig. 10c), CO mixing ratios ~105 ppb are observed near the location of cyclone and ~90 ppb near Ratnagiri coast, part of Karnataka, Andhrapradesh, region. Spatial distribution of CO at 316-mb level (Fig. 10d) shows merging of CO mixing ratios from low-pressure area with CO mixing ratios near the cyclone. CO mixing ratios >90 ppb are observed in this region. Spatial distribution of CO at 215 and 146 mb does not show enhanced values (figures not shown) near the location of cyclone or low-pressure area. Longitude–height cross-section (averaged over the BOB latitudes 8–22°N) shows (Fig. 10e) CO plume in the upper troposphere over the BOB longitudes (80–100°E). CO mixing ratios ~90 ppb are observed near 316-mb pressure level (Fig. 10e). Longitude–height cross-section of omega (averaged over 8–28°N latitudes) on November 15, 2007 is plotted in Fig. 10f. Strong convection

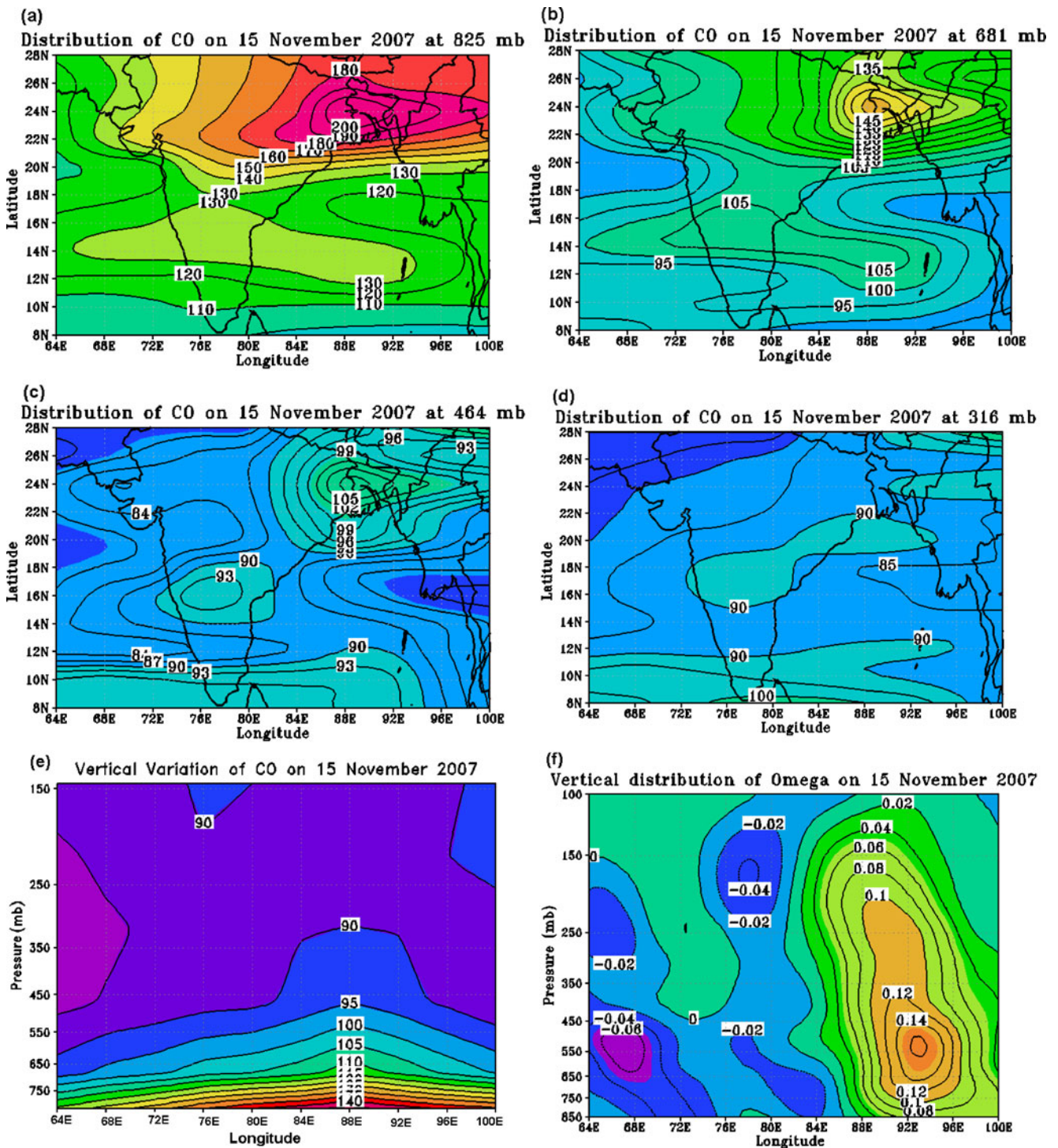


**Fig. 10** Spatial distributions of TES CO on November 15, 2007 at a 825 mb, **b** 681 mb, **c** 464 mb, and **d** 316 mb. **e** Longitude–height cross-section (mean for latitudes 8–22°N) of TES CO on November

15, 2007. **f** Longitude–height cross-section (mean for latitudes 8–22°N) of NCEP reanalysis vertical winds (omega) on November 15, 2007

( $\omega > 0.15$  Pa/s) from 825 to 200 mb is observed over the BOB longitudes. Vertical winds are stronger during the cyclone Mala ( $\omega > 0.2$  Pa/s; as can be seen in Fig. 4f), and they reach at the lower pressure levels (146 mb) as compared with cyclone Sidr. Hence, CO mixing ratios

~90 ppb are transported to 146 mb during cyclone Mala. During both the cyclones, ozone mixing ratios are transported from the lower troposphere to 316-mb level. Since CO has longer lifetime, it is transported at the higher altitude (~146 mb) during strong convection than that of ozone.

#### 4 Discussion

The spatial distribution of ozone and CO during two cyclones Mala and Sidr shows enhanced ozone and CO mixing ratios near the location of cyclone and low-pressure area, at the lower tropospheric pressure levels, and near the location of cyclone in the upper troposphere, indicating deep convective transport during cyclones. The days on which cyclone intensity was greatest, longitude–height cross-section of these pollutants shows their transport from the lower troposphere to 316-mb level (except during cyclone Mala, CO is lifted up to 146 mb). In general, CO mixing ratios  $\sim 90$  ppb and ozone  $\sim 70$ –100 ppb are observed near 316-mb level.

The evidence of vertical transport of CO in the upper troposphere due to convection during Indian summer monsoon is given by Kar et al. (2004); the CO maximum ( $\sim 120$  ppb) is observed near 316 mb. Model simulation (MOZART-4) also shows plume of high CO ( $\sim 100$  ppb) during monsoon season near the 15 km between latitudes 10 to 30°N (Park et al. 2009). Observed vertical transport of CO due to convection during super cyclones generally agrees with vertical transport of CO during monsoon season. From Geophysical Fluid Dynamics Laboratory–Global Chemical Transport Model (GCTM) model simulations, Phadnis et al. (2002) also reported maximum CO in the upper troposphere (near 316 mb) of the Indian Ocean, over the region stretching from the ITCZ to 20°N during winter monsoon (JFM) season. Phadnis et al. (2002) also reported that ozone pollution exhibits a tropical maximum at 316 mb during winter–spring monsoon. Hence, they suggested hypothesis that strong convection lifts transported surface pollution in to the upper troposphere over the equatorial Indian Ocean. Evidence of enhanced middle/upper tropospheric ozone via convective processes over the equatorial tropical region is also reported by Jenkins et al. (2008). Over the equatorial region (5°N–5°S), Jenkins et al. (2008) reported ozone mixing ratios  $\sim 100$ –120 ppb in the middle and upper troposphere during deep convection events. Regional Climate Model (RegCM3) simulations show episodic pulse of aerosols and trace gases being transported to the upper troposphere in the regions of deep convection (Jenkins et al. 2008). Similar results have been reported from observations and mesoscale simulations by Sauvage et al. (2007).

It is quite evident from Figs. 4, 5, 6, 7, 8, 9 and 10 that O<sub>3</sub> and CO are advected to  $\sim 316$ -mb pressure levels during the cyclone in the BOB region. Pollutants are lifted to higher altitudes during the cyclone occurring in the premonsoon season than the postmonsoon season, since convective activity is stronger during the premonsoon season. Amount of trapped gases especially ozone (in the lower troposphere) is high during cyclones occurring during the premonsoon than the postmonsoon season. From model simulations, Beig

and Ali (2006) reported that surface level ozone is high over the Indo-Gangetic plain during the premonsoon season as compared with the other seasons. General meteorological conditions prevailing over Indian region show warm weather, higher solar radiations, low humidity, and stagnant wind during the premonsoon season. Biomass burning activity is high during this period (March–April–May), it enhances the precursor pollutants. This is found to be favorable for the production of high ozone mixing ratios (Crutzen et al. 1995) and confinement of pollutants over this region.

In order to understand the circulation, winds have been analyzed at different pressure levels (1,000–100 mb) in the troposphere during the days of cyclones. Figure 11a–f shows winds at 500-, 300-, and 150-mb pressure levels, respectively, on a representative day of cyclones Mala (April 28, 2006) and Sidr (November 15, 2007). Cyclonic circulation is observed at all the pressure levels  $>300$  mb (as can be seen from Fig. 11a, b, d, e). Winds become anticyclonic near 200–150 mb. Anticyclonic circulation at 150 mb is quite evident in Fig. 11c, f. The anticyclone in the Upper Troposphere and Lower Stratosphere (ULTS) plays an important role in confining the pollutants in the Upper Troposphere. Pollutants may get trapped within the closed anticyclone near 100 mb. Recently, studies have reported that the Asian monsoon anticyclone traps pollutants, transported in the Upper Troposphere by large-scale monsoon convection (Randel and Park 2006; Park et al. 2009). From model simulations, Park et al. (2009) explained that CO mixing ratios are transported upward by deep monsoon convection, and some of the CO is advected vertically near the tropopause by large-scale upward circulation. This air then becomes trapped within the anticyclone. Dessler and Sherwood (2004) also suggested that overshooting convection is one of the mechanisms to transport constituents up to the tropopause in the anticyclone. The deep convective outflow in the tropics is typically near 12 km ( $\sim 200$  mb) (Folkins et al. 2000).

As evident from the above discussions, during these two super cyclones, pollutants (near the surface) are transported along with air masses to the location of cyclone that are from the surrounding regions (mostly Indo-Gangetic plains and South East Asia). Altitude–longitude distribution of these pollutants indicates that these pollutants are lifted upward to the upper troposphere due to strong convective activity during cyclone. The intense thunderstorm activity during cyclone also contributes in photochemical production of ozone (via production of NO<sub>x</sub>) in the upper troposphere. Strong convection (as observed from NCEP reanalysis vertical winds) over the BOB region confirms the vertical transport from the lower troposphere to the upper troposphere ( $\sim 200$ –146 mb). This air then may get trapped within the anticyclone near tropopause. High levels of tropospheric pollutant such as CO and hydrogen cyanide and HCN inside

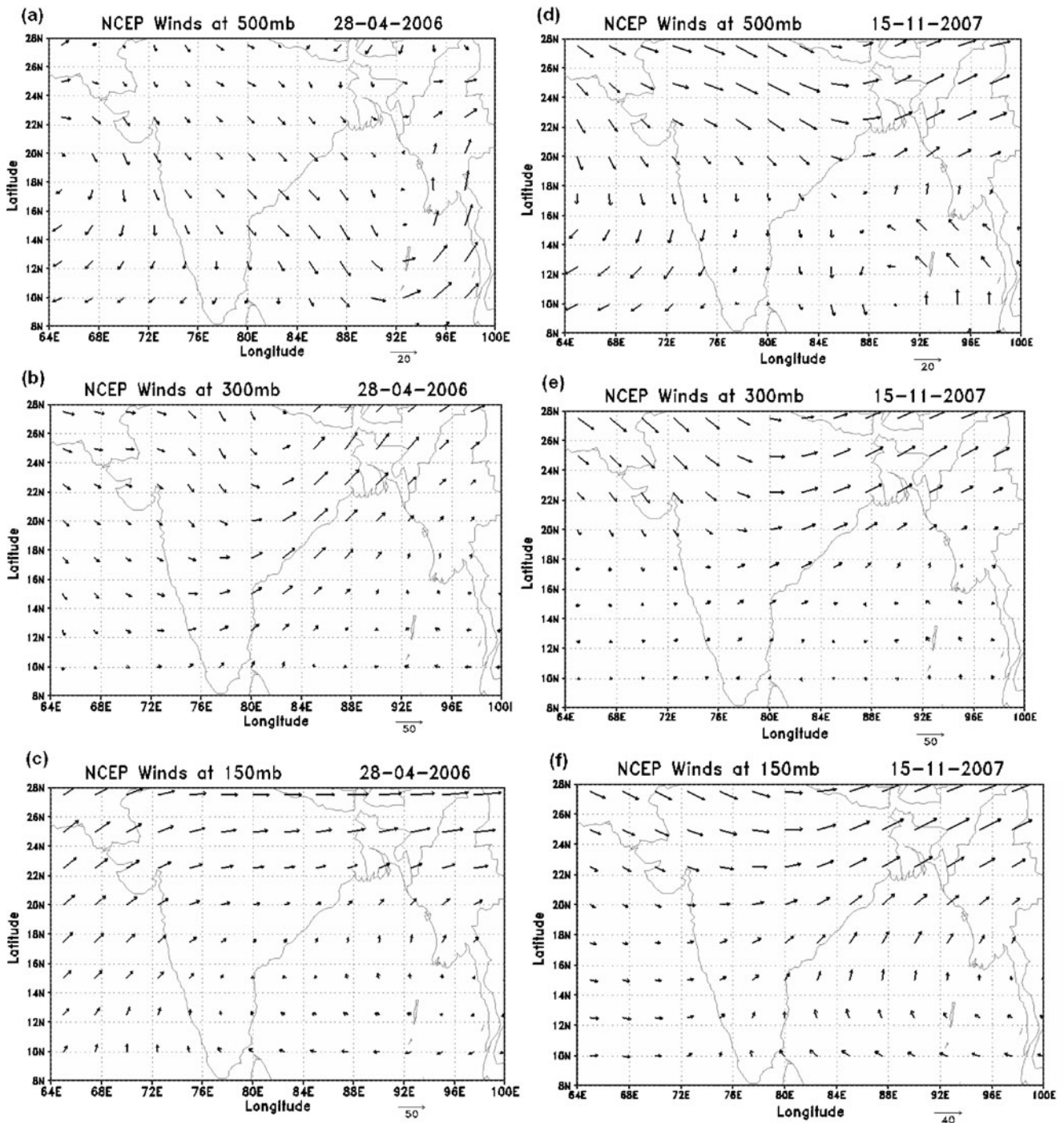


**Fig. 11** Spatial distributions of NCEP winds on April 28, 2006 at **a** 500 mb, **b** 300 mb, and **c** 150 mb and on November 15, 2007 at **d** 500 mb, **e**, 300 mb, and **f** 150 mb

the anticyclone are also reported by Li et al. (2005) and Park et al. (2008). These results are in agreement with us.

**5 Conclusions**

The analysis of vertical profiles of carbon monoxide (CO) and ozone retrieved from TES during two super cyclone

systems Mala (premonsoon) and Sidr (postmonsoon) provides an evidence of vertical transport of these pollutants to the upper troposphere. The spatial distribution of ozone and CO shows enhanced mixing ratios near the location of cyclone and low-pressure area at the lower tropospheric pressure levels (ozone: ~120–130 ppb and CO: ~140–150 ppb) and near the location of cyclone in the upper troposphere (ozone: ~90–95 ppb and CO: ~ 100–

110 ppb), indicating deep convective transport during cyclones. Longitude–height cross-section of these pollutants shows that these pollutants are lifted to the upper troposphere due to strong convection during cyclone. During the days on which cyclone intensity was greatest, longitude–height cross-section of these pollutants shows their transport from the lower troposphere to 316-mb level. CO mixing ratios ~90 ppb are observed near 146-mb level during the cyclone Mala and near 316-mb level during the cyclone Sidr. Ozone mixing ratios 60–100 ppb are observed near 316-mb level during both the cyclones. During cyclone Mala, CO is transported to higher altitudes as compared with ozone. The observed variation in vertical profiles of ozone and CO may be due to variations in their reactivity and variety of sources and sinks. Because of these differences, the vertical transport of CO is more evident than ozone.

NCEP reanalysis vertical winds confirm the vertical transport from the lower troposphere to the upper troposphere (~200–146 mb) over the BOB. Hence, it is proposed that strong winds gushing into cyclone bring the pollutants from surrounding region, which are then lifted upward due to strong convection during the cyclone. Anticyclone near 200- to 150-mb pressure level inhibits further vertical transport, and if get transported due to convection, they get trapped with the anticyclone.

**Acknowledgements** The authors thank the atmospheric science data center, NASA, for providing TES data. They thank John Worden, Jet Propulsion Laboratory (JPL), deputy principal investigator TES, California Institute of Technology, for the discussions on data quality. The authors also thank the anonymous reviewers for their critical comments and valuable suggestions, which helped in improving the scientific value of this research paper. The authors acknowledge the Ministry of Earth Sciences, Government of India, for the financial support and also thank Dr. B.N. Goswamy, Director IITM, for his encouragement.

## References

- Andreae MO, Artaxo P, Fische H, Freitas SR, Gregoire JM, Hansel A, Hoor P, Kormann R, Krejci R, Lange L, Lelieveld J, Lindinger W, Longo K, Peters W, de Reus M, Scheeren B, Silva Dias MAF, Ström J, van Velthoven PFJ, Williams J (2001) Transport of biomass burning smoke to the upper troposphere by deep convection in the equatorial region. *Geophys Res Lett* 28:951–954
- Beig G, Ali K (2006) Behavior of the boundary layer ozone and its precursors over a great alluvial plain of the world: Indo-Gangetic plain. *Geophys Res Lett* 33:L24813. doi:10.1029/2006GL028352
- Bellevue JL, Baray JL, Baldy S, Ancellet G, Diab R, Ravetta F (2007) Simulation of stratospheric to tropospheric transport during the tropical cyclone Marlene event. *Atmos Env* 41:6510–6526
- Cooper OR, Forster C, Parrish D, Trainer M, Dunlea E, Ryerson T, Hübner G, Fehsenfeld F, Nicks D, Holloway J, de Gouw J, Wreke C, Roberts JM, Flocke F, Moody J (2004) A case study of transpacific warm conveyor belt transport: influence of merging airstreams on trace gas import to North America. *J Geophys Res* 109:D23S08. doi:10.1029/2003JD003624
- Crutzen P, Groob J, Bruhl C, Muller R, Russell J III (1995) A reevaluation of the ozone budget with HALOE UARS data: no evidence for the ozone deficit. *Science* 268:705–708
- Das SS (2009) A new perspective on MST radar observations of stratospheric intrusions into troposphere associated with tropical cyclone. *Geophys Res Lett* 36:L15821. doi:10.1029/2009GL039184
- Dessler AE, Sherwood SC (2004) Effect of convection on the summertime extra tropical lower stratosphere. *J Geophys Res* 109:D23301. doi:10.1029/2004JD005209
- Dickerson RR, Li C, Li Z, Marufu LT, Stehr JW, McClure B, Krotkov N, Chen H, Wang P, Xia X, Ban X, Gong F, Yuan J, Yang J (2007) Aircraft observations of dust and pollutants over northeast China: insight into the meteorological mechanisms of transport. *J Geophys Res* 112:D24S90. doi:10.1029/2007JD008999
- Ding A, Wang T, Xue L, Gao J, Stohl A, Lei H, Dezhnev Jin Yu, Ren XW, Wei X, Qi Y, Liu J, Zhan X (2009) Transport of north China air pollution by midlatitude cyclones: case study of aircraft measurements in summer 2007. *J Geophys Res* 114:D08304. doi:10.1029/2008JD011023
- Folkens I, Oltmans SJ, Thompson AM (2000) Tropical convective outflow and near surface equivalent potential temperature. *Geophys Res Lett* 27(16):2549–2552. doi:10.1029/2000GL011524
- Ghude SD, Fadnavis S, Beig G, Polade SD, Van der A RJ (2008) Detection of surface emission hot spots, trends, and seasonal cycle from satellite-retrieved NO<sub>2</sub> over India. *J Geophys Res* 113:D20305, 1–13
- Hauglustaine D, Emmons L, Newchurch M, Brasseur G, Takao T, Matsubara K, Johnson J, Ridley B, Stith J, Dye J (2001) On the role of lightning NO<sub>x</sub> in the formation of tropospheric ozone plumes: a global model perspective. *J Atmos Chem* 38:3. doi:10.1023/A:1006452309388
- Henne S, Furger M, Nyeki S, Steinbacher M, Neining B, de Wekker SFJ, Dommen J, Spichtinger N, Stohl A, Prevot ASH (2004) Quantification of topographic venting of boundary layer air to the free troposphere. *Atmos. Chem Phys* 4:497–509
- Hess PG (2005) A comparison of two paradigms: The relative global roles of moist convective versus nonconvective transport. *J Geophys Res* 110:D20302. doi:10.1029/2004JD005456
- Indian Daily Weather Report, India Meteorological Department 2006 (2006) All India weather summaries of Indian Weather Review, Pune
- Indian Daily Weather Report, India Meteorological Department 2007 (2007) All India weather summaries of Indian Weather Review, Pune
- Intergovernmental Panel on Climate Change 2007 (2007) IPCC Fourth Assessment Report—Climate Change: The Physical Science Basis, Geneva, Switzerland, 104 pp
- Jenkins GS, Camara M, Seydi N (2008) Observational evidence of enhanced middle/upper tropospheric ozone via convective processes over the equatorial tropical Atlantic during the summer of 2006. *Geophys Res Lett* 35:L12806. doi:10.1029/2008GL033954
- Jourdain L, Worden HM, Worden JR, Bowman K, Li Q, Eldering A, Kulawik SS, Osterman G, Boersma KF, Fisher B, Rinsland CP, Beer R, Gunson M (2007) Tropospheric vertical distribution of tropical Atlantic ozone observed by TES during the northern African biomass burning season. *Geophys Res Lett* 34:L04810. doi:10.1029/2006GL028284
- Kar J, Bremer H, Drummond JR, Rochon YJ, Jones DBA, Zou FNJ, Liu J, Gille JC, Edwards DP, Deeter MN, Francis G, Ziskin D, Warner J (2004) Evidence of vertical transport of carbon monoxide from Measurements of Pollution in the Troposphere (MOPITT). *Geophys Res Lett* 31:L23105. doi:10.1029/2004GL021128
- Kiley CM, Fuelberg HE (2006) An examination of summertime cyclone transport processes during Intercontinental Chemical Transport Experiment (INTEX-A). *J Geophys Res* 111:D24S06. doi:10.1029/2006JD007115

- Kim YK, Lee HW, Park JK, Moon YS (2002) The stratosphere–troposphere exchange of ozone and aerosols over Korea. *Atmos Environ* 36 A:449–463
- Krishnamurti TN, Jha B, Rasch PJ, Ramanathan V (1997) A high resolution global reanalysis highlighting the winter monsoon. Part II: Transients and passive tracer transports. *Meteorol Atmos Phys* 64:151–171
- Krishnamurti TN, Chakraborty A, Martin A, Lau WK, Kim K-M, Sud Y, Walker G (2009) Impact of Arabian Sea Pollution on the Bay of Bengal winter monsoon rains. *J Geophys Res* 114:D06213. doi:10.1029/2008JD010679
- Kunhikrishnan T, Lawrence MG (2004) Sensitivity of NO<sub>x</sub> over the Indian Ocean to emissions from the surrounding continents and nonlinearities in atmospheric chemistry responses. *Geophys Res Lett* 31. doi:10.1029/2004GL020210
- Kunhikrishnan T, Lawrence MG, von Kuhlmann R, Richter A, Ladstätter-Weissenmayer A, Burrows JP (2004) Semiannual NO<sub>2</sub> plumes during the monsoon transition periods over the central Indian Ocean. *Geophys Res Lett* 31:L08110. doi:10.1029/2003GL019269
- Lelieveld JP, Crutzen J, Ramanathan V, Andreae MO, Brenninkmeijer CAM, Campos T, Cass GR, Dickerson RR, Fischer H, de Gouw JA, Hansel A, Jefferson A, Kley D, de Laat ATJ, Lal S, Lawrence MG, Lobert JM, Mayol-Bracero OL, Mitra AP, Novakov T, Oltmans SJ, Prather KA, Reiner T, Rodhe H, Scheeren HA, Sikka D, Williams J (2001) The Indian Ocean experiment: widespread air pollution from South and Southeast Asia. *Science* 291:1031. doi:10.1126/science.1057103
- Li Q, Jiang JH, Wu DL, Read WG, Livesey NJ, Waters JW, Zhang Y, Wang B, Filipiak MJ, Davis CP, Turquety S, Wu S, Park RJ, Yantosca RM, Jacob DJ (2005) Convective outflow of South Asian pollution: a global CTM simulation compared with EOS MLS observations. *Geophys Res Lett* 32:L14826. doi:10.1029/2005GL022762
- Liang Q, Jaeglé L, Jaffé DA, Weiss-Penzias P, Heckman A, Snow JA (2004) Long-range transport of Asian pollution to the northeast Pacific: seasonal variations and transport pathways of carbon monoxide. *J Geophys Res* 109:D23S07. doi:10.1029/2003JD004402
- Liu H, Jacob DJ, Bey I, Yantosca RM, Duncan BN, Sachse GW (2003) Transport pathways for Asian pollution outflow over the Pacific: interannual and seasonal variations. *J Geophys Res* 108 (D20):8786. doi:10.1029/2002JD003102
- Mahlman JD (1997) Dynamic of transport processes in the upper troposphere. *Science* 276(5315):1079–1083. doi:10.1126/science.276.5315.1079
- Miyazaki Y, Kondo Y, Koike M, Fuellberg HE, Kiley CM, Kita K, Takegawa N, Sachse GW, Flocke F, Weinheimer AJ, Singh HB, Eisele FL, Zondlo M, Talbot RW, Sandholm ST, Avery MA, Blake DR (2003) Synoptic-scale transport of reactive nitrogen over the western Pacific in spring. *J Geophys Res* 108 (D20):8788. doi:10.1029/2002/JD003248
- Park M, Randel WJ, Emmons LK, Bernath PF, Walker KA, Boone CD (2008) Chemical isolation in the Asian monsoon anticyclone observed in Atmospheric Chemistry Experiment (ACE-FTS) data. *Atmos Chem Phys* 8:757–764
- Park M, Randel WJ, Emmons LK, Livesey NJ (2009) Transport pathways of carbon monoxide in the Asian summer monsoon diagnosed from Model of Ozone and Related Tracers (MOZART). *J Geophys Res* 114:D08303. doi:10.1029/2008JD010621
- Phadnis MJ, Levy H II, Moxim WJ (2002) On the evolution of pollution from South and Southeast Asia during the winter–spring monsoon. *J Geophys Res* 107(D24):4790. doi:10.1029/2002JD002190
- Ramana MV, Ramanathan V (2006) Abrupt transition from natural to anthropogenic aerosol radiative forcing: observations at the ABC Maldives Climate Observatory. *J Geophys Res* 111:D20207. doi:10.1029/2006JD007063
- Randel WJ, Park M (2006) Deep convective influence on the Asian summer monsoon anticyclone and associated tracer variability observed with Atmospheric Infrared Sounder (AIRS). *J Geophys Res* 111:D12314. doi:10.1029/2005JD006490
- Sauvage B, Gheusi F, Thouret V, Cammas J-P, Duron J, Escobar J, Mari C, Mascart P, Pont V (2007) Medium-range mid-tropospheric transport of ozone and precursors over Africa: two numerical case-studies in dry and wet seasons. *Atmos Chem Phys Discuss* 7:4673–4703. doi:10.5194/acpd-7-4673-2007
- Streets DG, Waldhoff ST (2000) Present and future emissions of air pollutants in China: SO<sub>2</sub>, NO<sub>x</sub>, and CO. *Atmos Environ* 34:363–374
- Streets DG, Bond TC, Cannichael GR, Fernandes SD, Fu Q, He D, Klimont Z, Nelson SM, Tsai NY, Wang MQ, Woo J-H, Yarber KF (2003) An inventory of gaseous and primary aerosol emissions in Asia in the year 2000. *J Geophys Res* 108 (D21):8809. doi:10.1029/2002JD003093
- Tans PP, Fung IY, Takahashi T (1990) Observational constraints on the global atmospheric CO<sub>2</sub> budget. *Science* 247(4949):1431–1438
- Worden J, Kulawik SS, Shephard MW, Clough SA, Worden H, Bowman K, Goldman A (2004) Predicted errors of Tropospheric Emission Spectrometer nadir retrievals from spectral window selection. *J Geophys Res* 109:D09308. doi:10.1029/2004JD004522
- Worden J, Jones DBA, Liu J, Parrington M, Bowman K, Stajner I, Beer R, Jiang J, Thouret V, Kulawik S, Li F, Verma S, Worden H (2009) Observed vertical distribution of tropospheric ozone during Asian summertime monsoon. *J Geophys Res* 114: D13304. doi:1029/2008JD010560